MULTIPLE SIGNAL DETECTION AND PARAMETER ESTIMATION USING SENSOR ARRAYS WITH PHASE UNCERTAINTIES

D. Maiwald and U. Nickel

FGAN–FFM
Neuenahrer Str. 20, D–53343 Wachtberg

ABSTRACT

In this paper a procedure is outlined for performing both sensor array calibration and signal detection/direction of arrival estimation simultaneously. The source directions are unknown. Sensor array calibration is done using a least squares technique. Signal detection and direction of arrival estimation is performed by a multiple test procedure based on F–tests. The algorithm is studied by simulations and by numerical experiments with data measured by an experimental radar array with 8 elements.

1 INTRODUCTION

In this paper the calibration of an array of sensors is investigated for a phased array radar application. The sensivity of high resolution methods to calibration errors is well known. Conventionally, in radar applications calibration is done by insertion of a test signal, e.g by using sources in known positions. However, to measure the complete array manifold over the desired field of view is time consuming and even impossible in certain situations. Furthermore, model errors can be slowly time varying and direction dependent. Therefore, auto–calibration of sensor arrays using a suitable model and parameter estimation techniques is of great interest. In recent years a number of algorithms have been proposed to overcome the sensivity of high resolution methods to model errors, see e.g. [6], [8], [7].

In this contribution a model taking account of sensor phase uncertainties is used. We investigate the influence of the errors on the performance of a recently discussed multiple test procedure for estimating the number of signals. Array calibration is done by a least squares technique. A procedure is outlined for performing both sensor array calibration and signal detection/direction of arrival (DOA) estimation simultaneously. The algorithm is studied by simulations and is applied to data measured by an experimental radar array. Finally, it is shown how the performance of the Capon method improves by using the calibration technique.

2 DATA MODEL

A conventional propagation-reception model is used. Signals additively disturbed by noise are measured by sensors of a planar array at positions $\underline{r}_1, \ldots, \underline{r}_N$. In a narrowband situation the N dimensional snapshot vectors $\underline{x}(t)$ collecting the outputs of the sensors in complex envelope notation can be described by covariance matrices

$$\mathbf{R} = \tilde{\mathbf{H}}\mathbf{S}\tilde{\mathbf{H}}^* + \sigma^2\mathbf{I} \quad \text{with} \quad \tilde{\mathbf{H}} = \mathbf{G}\mathbf{H}. \qquad (1)$$

Temporally white, but spatially correlated stationary signals $s_1(t), \ldots, s_M(t)$ in unknown directions are assumed with covariance matrix $\mathbf{S}$. M is the number of signals, the symbol * indicates the hermitian operation. Temporally and spatially white stationary receiver noise is assumed with variance σ^2. $\mathbf{I}$ is the $(N \times N)$ identity matrix. The propagation–reception situation is described by the $(N \times M)$ matrix $\mathbf{H} = [\underline{d}_1, \ldots, \underline{d}_M]$ with the phase vectors $\underline{d}_i = [e^{-j\underline{k}_i'\underline{r}_1}, \ldots, e^{-j\underline{k}_i'\underline{r}_N}]'$. $\underline{k}_i$ is the wavenumber vector corresponding to the ith signal and is parameterized by the DOA of the ith signal, by the carrier frequency, and by the wave velocity. For a planar array, $\underline{k}_i$ consists of two components $[k_{x,i},\, k_{y,i}]'$. Let us collect all wavenumbers in one vector $\underline{\vartheta}$. $\mathbf{G}$ is a complex diagonal matrix whose diagonal entry $g_n = e^{j\phi_n} \quad (n = 1, \ldots, N)$ is the complex response of sensor n. This means that we are dealing with phase calibration only. We collect the sensor phases in one vector $\underline{\phi}$ and the elements g_n in a vector $\underline{g} = (g_1, \ldots, g_N)'$. The covariance matrix of sensor outputs is estimated by $\hat{\mathbf{R}} = \frac{1}{K}\sum_{k=1}^{K} \underline{x}(t_k)\underline{x}^*(t_k)$.

3 PROCEDURES

3.1 Calibration

In this paper we use a least squares technique ([1],[4]) for estimating the sensor phases in a narrowband situation. The idea is to fit the parametric model of the covariance matrix $\mathbf{R}(\underline{\vartheta}, \underline{\phi}, \mathbf{S}, \sigma^2)$ to its estimate $\hat{\mathbf{R}}$

$$q(\underline{\vartheta}, \underline{\phi}, \mathbf{S}, \sigma^2) = \operatorname{tr}\left\{\hat{\mathbf{R}} - \mathbf{R}\right\}^2. \qquad (2)$$

Minimization of $q(\underline{\vartheta}, \underline{\phi}, \mathbf{S}, \sigma^2)$ over the elements of the signal covariance matrix and the noise variance yields explicit solutions:

$$\mathbf{S} = \tilde{\mathbf{H}}^{\#}\left(\hat{\mathbf{R}} - \tilde{\sigma}^2\mathbf{I}\right)\tilde{\mathbf{H}}^{\#^*}, \quad \tilde{\mathbf{H}}^{\#} = (\tilde{\mathbf{H}}^*\tilde{\mathbf{H}})^{-1}\tilde{\mathbf{H}}^*$$

with

$$\tilde{\sigma}^2 = \frac{\mathrm{tr}\left\{\mathbf{P}^{\perp}\hat{\mathbf{R}}\right\}}{N - M}, \quad \mathbf{P} = \tilde{\mathbf{H}}\tilde{\mathbf{H}}^{\#}, \quad \mathbf{P}^{\perp} = \mathbf{I} - \mathbf{P}.$$

These solutions can be put into criterion (2) and one obtains:

$$\tilde{q}(\underline{\vartheta}, \underline{\phi}) = \mathrm{tr}\left\{\mathbf{C}^2 - \mathbf{PCPC}\right\}, \quad \mathbf{C} = \hat{\mathbf{R}} - \tilde{\sigma}^2\mathbf{I}. \tag{3}$$

We are left with a minimization problem over the elements of $\underline{\vartheta}$ and $\underline{\phi}$. In the next paragraph it is described how initial direction estimates $\hat{\underline{\vartheta}}_{ini}$ of $\underline{\vartheta}$ are obtained. Then, we are using the scoring method to minimize $\tilde{q}(\hat{\underline{\vartheta}}_{ini}, \underline{\phi})$ over the calibration phases $\underline{\phi}$.

3.2 Initial DOA Estimates and F Test

Multiple F–tests are useful for estimation of the number of signals impinging on the array, see e.g. [3]. A stepwise test procedure is constructed, starting with a test for one signal present. If one decides that at least one signal is present, the parameters of interest for the first signal are estimated. Then, we test for a second signal, and so on. The test statistic for the first signal is given by

$$F_1(\vartheta_1, \hat{\underline{\phi}}) = \frac{\mathrm{tr}\{\mathbf{P}\hat{\mathbf{R}}\}}{\mathrm{tr}\{\mathbf{P}^{\perp}\hat{\mathbf{R}}\}}\frac{\nu_2}{\nu_1} \tag{4}$$

with $\nu_1 = K(2 + \eta)$, $\nu_2 = K(2N - (2 + \eta))$, see e.g. [3]. The parameter η is determined by the number of nonlinear parameters for one signal, i.e. number of elements of the corresponding wavenumber vector. For line arrays we use $\eta = 1$, for the planar array one has $\eta = 2$. The distribution of (4) can be approximated by a central F distribution with ν_1 and ν_2 degrees of freedom if no signal is present. $\hat{\underline{\phi}}$ denotes estimates of the calibration phases. If the maximum of (4) exceeds a test threshold, it is decided that at least one signal is present and the argument of the maximum is an estimate of the DOA of the first signal. The pattern given by (4) as a function of the elements of $\underline{k}_1$ is very similar to a conventional beamformer pattern. It is known that the mainlobe of a beamformer pattern is very robust to calibration errors described by the matrix $\mathbf{G}$. Therefore, the estimate of the elements of $\underline{k}_1$ will be a good initial estimate for a calibration step based on (3) even if calibration errors are present. Expression (4) is an estimate of the ratio of signal power and noise power. If we have decided that one signal is present, we are interested if the data contain a second signal. As a test criterion a ratio of powers can be used. The numerator of this ratio is an estimate of the power of a signal that is orthogonal to the first signal. The denominator is an estimate of the noise power assuming that two signals are present. Again, it is possible to a use F statistics for testing the hypothesis of interest. The procedure can be extended to more than two signals. We remark that the test thresholds are determined by the so–called multiple level of the test procedure. In all numerical experiments we control this level to 5%. Details can be found e.g. in [2].

3.3 Algorithm

At the start of the algorithm initial values of the sensor phases have to be defined. In simulations, these values are drawn from a uniform distribution. For measured data the initial phases are chosen to be zero. Then, in each stage of the test procedure the complete procedure consists first of obtaining initial estimates of the directions of arrival. Then, a calibration step using (3) is performed. Finally, it can be tested if the corresponding signal is present using the estimated sensor phases. This means that one calibration step and two DOA estimation steps are executed. One could perform iteratively several calibration and direction estimation steps before testing. But, numerical experiments show that there is almost no change in the estimated directions and calibration phases after the first iteration. At the end of the procedure a number of signals is detected and the corresponding wavenumbers are estimated. Sensor phase estimates are available.

4 NUMERICAL EXPERIMENTS

4.1 Artificial Data

Pseudo–random matrices for model (1) are generated with K degrees of freedom. We simulate a planar array with the same element positions as are used by the FFM–DESAS array described in the next subsection. Two signals are present with $\underline{k}_1/k_{max} = [0\,0]'$ and $\underline{k}_2/k_{max} = [0.1228, 0.1228]'$ with $k_{max} = 2\pi/\lambda$. The signals can not be separated by conventional beamforming. The nominal sensor phase is zero. Sensor phases are perturbed and are uniformly distributed on the intervall $(-\beta, \beta)$. The powers of the signals are equal and are changed from 21 dB down to -6 dB in 3 dB steps. For each power configuration 200 complex Wishart distributed pseudo random matrices are generated and the test procedure is executed for each of these matrices. After the experiment we determine for each power configuration how often the correct number of signals has been detected. We perform this experiment for Wishart matrices with $K = 25$, $K = 50$, and $K = 100$ degrees of freedom. In Fig. 1 the result of the experiment is presented for $\beta = 20°$. In this figure the line with the stars corresponds to a case where no calibration is done. The results are not greatly dependent on β. We have obtained very similar results for $\beta = 60°$. The estimated

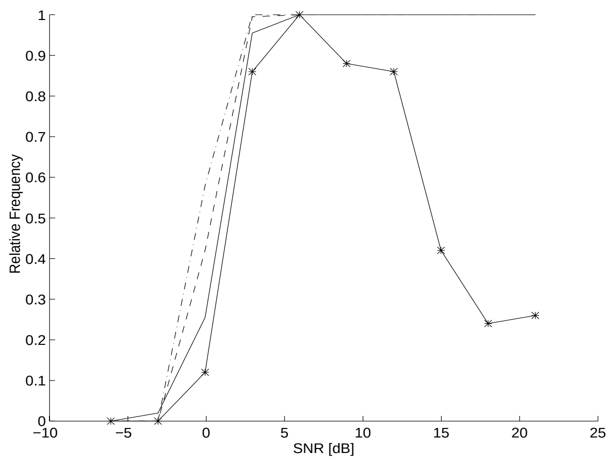

Figure 1: Correct decision of test procedure for different degrees of freedom; $K = 25$: solid line; $K = 50$: dashed line; $K = 100$: dashed dotted line; line with stars: no calibration.

wavenumbers are shown in Fig. 2 for signal powers of $3\ dB$. The circle corresponds to the $3\ dB$ beamwidth of the antenna. Clearly, the algorithm can separate the two signals.

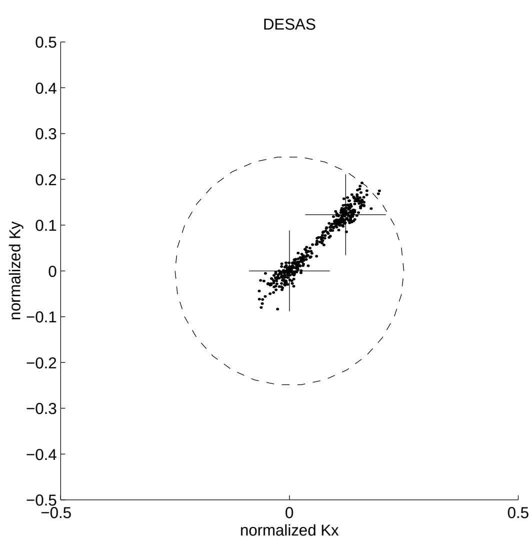

Figure 2: Estimated wavenumbers: $K = 25$, $SNR = 3\ dB$.

4.2 Measured Data

The algorithm is applied to data measured by the FFM–DESAS experimental array at S band [5]. The transmitting part of the systems is build up by two antennas which can be fed with a monochromatic signal and a doppler shifted monochromatic signal. One of the antennas can be moved to different directions, the other antenna is fixed. The antennas are mounted on equal height. The receiving part of the system consists of a planar 8 element array. Each element is equipped with a receiving channel up to A/D conversion where the baseband signal is sampled. The elements are distributed on a circle with one element in the centre. Measured data are preprocessed, i.e. an offset vector and a focussing matrix are applied. The focussing matrix is a diagonal matrix with elements collected in a focussing vector $\underline{c}$. Both the offset and the focussing vector are determined with the fixed antenna turned on. The monochromatic signal is used and data vectors $\underline{z}(t_k)$ $(k = 1, \ldots, K_1; K_1 = 500)$ are collected. Using these data the offset vector $\underline{o}$ and the vector $\underline{c}$ with elements

$$c_i = \left(\frac{1}{K_1} \sum_{k=1}^{K_1} \frac{1}{z_1(t_k)} \underline{z}(t_k) \right)^{-1}, \quad i = 1, \ldots, N$$

are determined. Application of these vectors to the data $\underline{x}(t) = \mathrm{diag}(\underline{c})(\underline{z}(t) - \underline{o})$ sets the origin in the direction of the transmitting antenna. The offset and the focussing matrix are applied to all measured data presented in the sequel. 45 data pieces with $K = 20$ snapshots each are collected and analyzed. Both antennas are turned on. For each data piece the calibration and the detection/estimation procedure is executed. The maximum possible number of signals is 6. Fig. 3 shows the estimated wavenumbers given by the procedure. At most 4 signals are detected. The two signals in the circle in Fig. 3 correspond to the two transmitting antennas. The third signal at the upper edge of the figure is due to an antenna ambiguity. A calibration of sensor phases is desired e.g for the Capon method as described next.

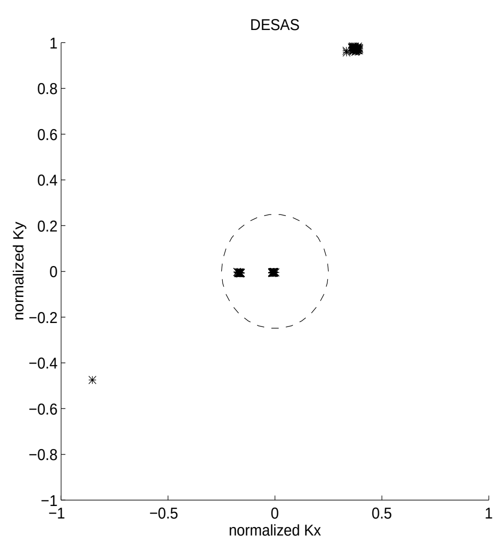

Figure 3: Estimated wavenumbers for measured data.

4.3 Capon Method

Capon–type methods or Projection methods are very sensitive to calibration errors. The application of superresolution methods to phased array radar data is described e.g. in [5]. Here, we use the Capon method to demonstrate the effects of calibration. The Capon method searches the spectrum $1/(\underline{d}(\underline{k})^* \hat{\mathbf{R}}^{-1} \underline{d}(\underline{k}))$ for peaks. This is shown in Fig. 4 for the same data set as used in section 4.2. Only the preprocessing and no calibration based on (3) is done. Actually, we have to search a 3–dimensional surface for peaks. Because $k_y \approx 0$ for both signals, we plot only k_x–patterns. The procedure used in section 4.2 gives a calibration vector for each data piece. The mean of these vectors is used to calibrate the antenna and the Capon method is applied again, see Fig. 5. Comparing Fig. 4 and 5 one sees the improvement when the calibration vector is used. The two signals can be resolved by the superresolution method which is not possible without calibration.

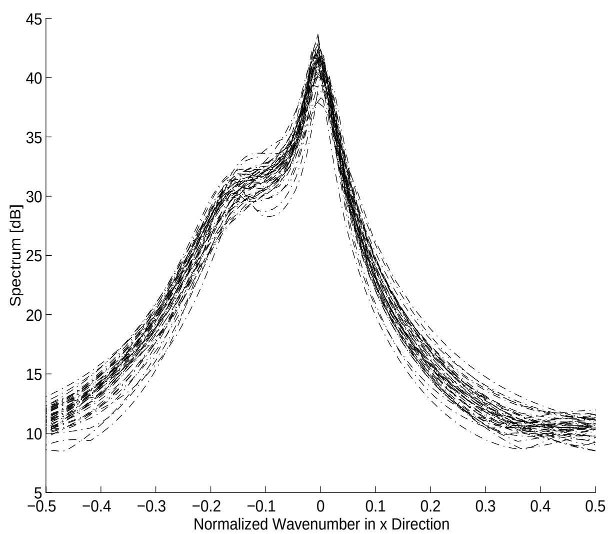

Figure 4: Capon spectrum for measured data; no calibration; $K = 20$; 45 trials.

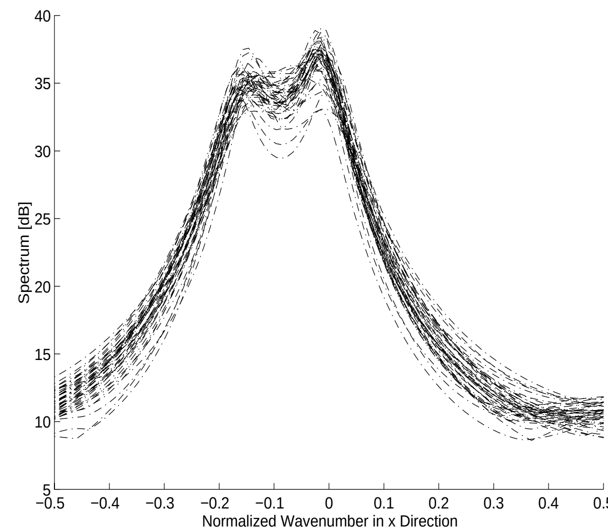

Figure 5: Capon spectrum for measured data; with calibration; $K = 20$; 45 trials.

5 CONCLUSIONS

In this paper, calibration of a sensor array and signal detection/DOA estimation are done simultaneously. The number of signals is not correctly estimated by a multiple test procedure without sensor array calibration. Simulations show that the performance of the test procedure can be significantly improved using calibration. The proposed algorithm is successfully applied to measured radar data.

References

[1] D. Kraus, G. Schmitz, and J.F. Böhme. Least squares estimates for source location and asymptotic behaviours. In *Proc. 5th European Signal Processing Conf., Signal Processing V: Theories and Applications*, pages 649–652, Barcelona, 1990.

[2] D. Maiwald. *Breitbandverfahren zur Signalentdeckung und –ortung mit Sensorgruppen in Seismik– und Sonaranwendungen.* Dr.–Ing. thesis, Ruhr-Universität Bochum, 1995 (in German).

[3] D. Maiwald and J. F. Böhme. Multiple testing for seismic data using bootstrap. In *Proc. IEEE Int. Conf. Acoust., Speech, Signal Processing*, pages VI89–VI92, Adelaide, 1994.

[4] D. Maiwald, D. Kraus, and J. F. Böhme. Signal parameter estimation for seismic data. In *Proc. 6th European Signal Processing Conf., Brüssel*, pages 1801–1804, 1992.

[5] U. Nickel. Application of array signal processing to phased array radar. In *Proc. 4th European Signal Processing Conf.; Signal Processing IV: Theory and Applications*, pages 467–474, 1988.

[6] Y. Rockah and P. M. Schultheiss. Array shape calibration using sources in unknown locations–part I: Far–field sources. *IEEE Trans. Acoust., Speech, Signal Processing*, 35:286–299, 1987.

[7] M. Viberg and A. L. Swindlehurst. A bayesian approach to auto–calibration for parametric array signal processing. *IEEE Trans. Signal Processing*, 42:3495–3507, 1994.

[8] A. J. Weiss and B. Friedlander. Array shape calibration using sources in unknown locations–a maximum likelihood approach. *IEEE Trans. Acoust., Speech, Signal Processing*, 37:1958–1966, 1989.